The Intermembrane Space Loop of Subunit *b* (*4*) Is a Major Determinant of the Stability of Yeast Oligomeric ATP Synthases†

Théodore Weimann,‡ Jacques Vaillier, Bénédicte Salin, and Jean Velours*

Université de Bordeaux 2, Institut de Biochimie et Génétique Cellulaires, CNRS UMR 5095, 1 rue Camille Saint Saëns, 33077 Bordeaux, France

Received October 5, 2007; Revised Manuscript Received December 27, 2007

ABSTRACT: The involvement of the *b*-subunit, subunit *4* in yeast, a component of the peripheral stalk of the ATP synthase, in the dimerization/oligomerization process of this enzyme was investigated. Increasing deletions were introduced by site-directed mutagenesis in the loop located in the mitochondrial intermembrane space and linking the two transmembrane (TM) segments of subunit *4*. The resulting strains were still able to grow on nonfermentable media, but defects were observed in ATP synthase dimerization/oligomerization along with concomitant mitochondrial morphology alterations. Surprisingly, such defects, already depicted in the absence of the so-called dimer-specific subunits *e* and *g*, were found in a mutant harboring a full amount of subunit *g* associated to the monomeric form of the ATP synthase. Deletion of the intermembrane space loop of subunit *4* modified the profile of cross-linking products involving cysteine residues belonging to subunits *4*, *g*, *6*, and *e*. This suggests that this loop of subunit *4* participates in the organization of surrounding hydrophobic membranous components (including the two TM domains of subunit *4*) and thus is involved in the stability of supramolecular species of yeast ATP synthase in the mitochondrial membrane.

The F_oF_1-ATP synthase is a molecular rotary motor that is responsible for aerobic synthesis of ATP. It exhibits a headpiece (catalytic sector), a base piece (membrane sector), and two connecting stalks. The F_1 sector is a water-soluble unit retaining the ability to hydrolyze ATP when in soluble form. F_o is embedded in the membrane and is mainly composed of hydrophobic subunits forming a specific proton-conducting pathway. When the F_1 and F_o sectors are coupled, the enzyme functions as a reversible H^+-transporting ATPase or ATP synthase (*1–4*). The two connecting stalks are constituted of components from F_1 and F_o. The central stalk is a part of the rotor of the enzyme. The second stalk (also called the peripheral stalk), which is part of the stator, connects F_1 and hydrophobic membranous components of the enzyme via a thin region which has been recently crystallized (*5*). High-resolution X-ray crystallographic data have led to solving the structure of F_1 from different species (*6–9*). In addition, Stock et al. (*10*) reported the 3.9 Å resolution X-ray diffraction structure of the *Saccharomyces cerevisiae* F_1 associated with a c_{10}-ring oligomer.

As shown in detergent extracts, using native gels, for a large range of species including yeast, mammalian, and plants, mitochondrial F_oF_1-ATP synthases adopt oligomeric structures (*11–13*). Moreover, low-resolution structural data obtained from single particle electron microscopy analyses are available for dimeric forms in detergent extracts (*14–16*). On the other hand, association of ATP synthase monomers in the mitochondrial membrane has been reported on the basis of chemical (*17, 18*) and *in vivo* (*19*) cross-linking experiments. Recently, atomic force microscopy experiments have revealed the oligomeric state of the enzyme in the yeast inner mitochondrial membrane (*20*).

Ten different subunits compose the mitochondrial F_o (*11, 21–23*) among which only three are present in the bacterial and chloroplastic enzyme. Among the seven additional subunits not present in bacterial and chloroplast ATP synthases, two small hydrophobic proteins, subunits *e* and *g*, are not involved in ATP synthesis function but rather in the dimerization/oligomerization of the mitochondrial ATP synthase (*11, 24*). Indeed, the absence of subunits *e* and *g* dramatically decreases the stability of ATP synthase as shown by BN-PAGE experiments. Recent data based on cross-linking studies and FRET experiments led to the conclusion that subunits *e* and *g* stabilize the ATP synthase dimers in detergent extracts and participate in the enzyme oligomerization in association with components of the peripheral stalk (*25, 26*). The evidence that two peripheral stalks of dimeric ATP synthases are in close proximity was also recently brought by electron microscopy experiments and single particle analyses of ATP synthase dimers from several sources (*14–16*). It has been proposed that such a proximity could drive the inhibitory activity of the peptide IF_1. Involvement of this peptide in dimerization process of ATP synthases has been observed for the mammalian but not for the yeast enzyme (*27, 28*).

† This work was supported by grants from the CNRS [ACI Biologie cellulaire, moléculaire et structurale (BCMS) and UMR5095], Université Victor Segalen Bordeaux 2, and the Conseil Régional d'Aquitaine. T.W. held a research grant from the Ministère de la Recherche et la Technologie.

* To whom correspondence should be addressed. Tel: 33 5 56999001. Fax: 33 5 56999010. E-mail: jean.velours@ibgc.u-bordeaux2.fr.

‡ Present address: Laboratoire de Bioénergétique Fondamentale et Appliquée, Université Joseph Fourier Grenoble 1, INSERM U-884, BP 53, 38041 Grenoble Cedex 9, France.

10.1021/bi702000g CCC: $40.75
Published on Web 02/23/2008

Early electron microscopy observations led to the proposal of a role for ATP synthase oligomerization in the morphogenesis of the inner mitochondrial membrane (*29, 30*). Surprisingly, yeast mitochondria devoid of either subunit *e* or subunit *g* were found to harbor numerous digitations with mitochondrial cristae appearing as elongated sheets and "onion-like structures" (*24, 31*). Furthermore, *in vivo* cross-linking of oligomeric ATP synthases using a subunit γ-DsRed fusion protein has led to a similar abnormal cristae topology (*19*). These observations, arguing for a physiological role of ATP synthase oligomerization in the biogenesis and/or maintenance of cristae morphology, are sustained by structural analyses of dimeric ATP synthases. Indeed, in detergent extracts, electron microscopy showed that the axes of two monomers of dimeric species of ATP synthases form an angle (*14–16*). This relates these supramolecular structures to the bending of the inner membrane in mitochondrial cristae.

The present work is focused on the involvement of the *b*-subunit (subunit *4* in yeast), which is a main component of the peripheral stalk, in the dimerization/oligomerization of the ATP synthase. Previous data have determined that in a yeast strain devoid of the subunit *4* N-terminal part, which contains the first transmembrane segment (TM1),[1] subunit *g* is absent, and the ATP synthase is still functional but does not dimerize or oligomerize (*32*). On the basis of the absence of subunit *g* in this mutant and on cross-linking experiments, it was hypothesized that the TM1 of the mitochondrial *b*-subunit could interact with subunit *g*. The purpose of the present paper was to introduce alterations in the vicinity of TM1 to modify this interaction with subunit *g*. In the context of increasing deletions in the loop linking the two membrane-spanning segments of subunit *4* (*b*), we report a decrease in the ATP synthase oligomer amount in detergent extracts whereas subunit *g* was still associated to the enzyme and modifications of the environment of some residues in subunits *4*, *g*, *6*, and *e*. These defects are correlated with a lamellarization of mitochondrial cristae.

EXPERIMENTAL PROCEDURES

Materials. Digitonin from Sigma was recrystallized as in ref *33*. Oligonucleotides were purchased from MWG-BIOTECH. All other reagents were of reagent grade quality.

Yeast Strain Mutagenesis. The *ATP4* gene cloned in the low copy shuttle vector pRS313 was the target for a PCR-based mutagenesis (*34*). When necessary, two rounds of mutagenesis led to the twice mutated *ATP4* gene, harboring a deleted and substituted sequence. Mutations were verified by sequencing. Plasmids were used to transform the *S. cerevisiae* strain PVY10 (MATα, *met6*, *ura3*, *his3*, *atp4*::*URA3*) derived from the D273-10B/A/H/U (MATα, *met6*, *ura3*, *his3*) after deletion of the *ATP4* gene (*35*). The control PVY162 strain resulted from such a transformation using pRS313 harboring the wild-type *ATP4* gene. Mutant strains were named after the deleted domain as illustrated in Figure 1. In the strain *4*ΔTM1 the altered *ATP4* gene was inserted at its chromosomal locus (*32*).

[1] Abbreviations: CN-PAGE, clear-native polyacrylamide gel electrophoresis; SDS−PAGE, sodium dodecyl sulfate−polyacrylamide gel electrophoresis; NEM, *N*-ethylmaleimide; PMSF, phenylmethanesulfonyl fluoride; TM, transmembrane.

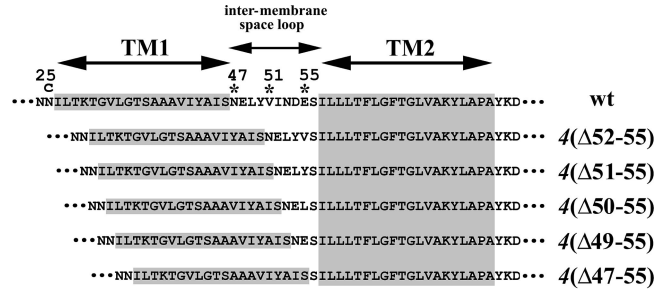

FIGURE 1: Primary structures of wild-type and mutant subunits *4*. Only the sequences containing the two transmembrane segments TM1 and TM2 (gray portions) flanking the intermembrane space loop 47–55 of subunit *4* are shown. The numbering of amino acid residues is that of the wild-type sequence of yeast (wt). Key: C, cysteine residue substituting the asparagine 25 in some strains; *, most conserved amino acid positions.

Biochemical Procedures. Cells were grown aerobically at 28 °C in a complete liquid medium containing 2% lactate as carbon source (*36*). The generation of *petite* mutants in cultures was measured on glycerol plates supplemented with 0.1% glucose. Mitochondria were prepared from protoplasts as previously described (*37*). Protein amounts were determined according to Lowry et al. (*38*) in the presence of 5% SDS using bovine serum albumin as standard. ATP/O ratios were determined as in ref *39*. The ATPase activity with and without oligomycin was measured at pH 8.4 in the presence of 0.375% Triton X-100 to remove the endogenous IF_1 inhibitor (*40*). For cross-linking experiments with $CuCl_2$, mitochondria were washed twice in 0.1 M mannitol and 50 mM HEPES, pH 7.0, suspended in the same buffer at a protein concentration of 5 mg/mL, and incubated in the presence or absence of 1 mM $CuCl_2$ for 30 min at 4 °C. In control experiments, mitochondrial suspensions were incubated in the same conditions with 5 mM NEM. The disulfide bond formation by $CuCl_2$ was stopped by the addition of 5 mM EDTA and 5 mM NEM.

Electrophoretic and Western Blot Analyses. SDS gel electrophoreses were done as described (*41, 42*) using a *T%* = 12 in both cases (where *T%* is the total percentage of acrylamide and bisacrylamide prior to polymerization reaction). Western blot analyses were conducted using nitrocellulose membranes (Membrane Protean BA83, 0.2 μm, from Schleicher & Schuell), and polyclonal antibodies against subunits *4*, *e*, *g*, *i*, and *6* were used as described previously (*43*). Antibodies against subunit *k* were a gift from Dr. Rosemary Stuart, Department of Biological Sciences, Marquette University, Milwaukee, WI 53233. When necessary, stripping of primary and secondary antibodies was carried out by incubation of the membrane in 2% SDS, 0.1 M β-mercaptoethanol, and 62.5 mM Tris-HCl, pH 6.7, for 30 min at 50 °C, followed by a classical antibody hybridization protocol. Peroxidase activity of secondary antibodies was visualized by incubating the membrane for 1 min in 0.4 mM coumaric acid, 2.5 mM luminol, 0.0165% (v/v) H_2O_2, and 0.1 M Tris-HCl, pH 8.5. Subunit *g* content was determined by densitometry using the Gnome program on images acquired with a CCD-based camera (Syngen). CN-PAGE experiments were done as described in ref *44*. Mitochondria (0.5 mg of protein) were incubated for 30 min at 4 °C with 50 μL of digitonin dissolved in 150 mM potassium acetate, 2 mM aminocaproic acid, 15% glycerol, 1 mM PMSF, and 30 mM HEPES, pH 7.4 (adapted from ref *11*), at the

Table 1: Phenotypic Analyses of Yeast Mutants[a]

mutant	doubling time (min)	*petite* mutants (%)	ATPase activity: μmol of P_i min^{-1} (mg of protein)$^{-1}$	ATPase activity: % oligomycin sensitivity
PVY162	204	17	4.40 ± 0.47	77
*4*Δ(52–55)	230	16	3.76 ± 0.10	65
*4*Δ(51–55)	230	18	2.91 ± 0.07	53
*4*Δ(50–55)	244	17	3.64 ± 0.10	66
*4*Δ(49–55)	221	16	3.95 ± 0.09	49
*4*Δ(47–55)	424	35	3.07 ± 0.16	8
*4*ΔTM1[b]	208	31	5.00 ± 0.10	56

[a] The control strain was the PVY162 strain. It was obtained from the PVY10 strain (*35*) deleted in the ATP4 gene and complemented with the low copy shuttle vector pRS313 harboring the wild-type ATP4 gene. The conversion into *petite* mutants in cultures was measured on glycerol plates supplemented with 0.1% glucose. Mitochondria were prepared from protoplasts. Data of time generation are from typical experiments. ATPase activities and the sensitivity to the F_o inhibitor oligomycin (6 μg/mL) were measured at pH 8.4 in the presence of 0.375% Triton X-100 (w/v) to remove the IF_1 inhibitor. [b] From ref *32*.

indicated digitonin to protein ratios. The extracts were centrifuged at 4 °C for 30 min at 24000*g*, and aliquots containing 150 μg of protein were loaded onto a 3–13% polyacrylamide slab gel. After electrophoresis the gel was incubated in 5 mM ATP, 5 mM $MgCl_2$, 0.05% lead acetate, and 50 mM glycine−NaOH, pH 8.4, to reveal the ATPase activity (*45, 46*). The white precipitate resulting from ATP hydrolysis was removed in acidic medium, and the gel was stained by Coomassie Brilliant Blue.

Ultrastructural Studies. Freezing and freeze substitution of yeast cell pellets were carried out as previously described (*24*). Grids were examined at 120 kV using a Philips Tecnai 12 Biotwin.

RESULTS

Mutant Cell Growth and ATPase Function. The topology of subunit *4* (the bovine *b*-subunit) is conserved among the mitochondrial *b*-subunits. It consists in a large matricial C-terminal domain, two transmembrane domains (TM1 and TM2) connected by a short loop in the intermembrane space, and a small matricial N-terminal domain. The role of the enlarged N-terminal domain, i.e., containing TM1, has been studied previously (*32*). Here we focused on the loop linking the two membrane-spanning segments of subunit *4*. This loop is predicted to stretch from residue 47 to residue 55 (using TMpred server) and is localized in the intermembrane space (*47*). Using site-directed mutagenesis, deletions of increasing size were introduced to shorten the loop (Figure 1). Phenotypic analyses of yeast mutant strains and mitochondria are presented in Table 1. *4*Δ(47–55) was the only deletion for which the generation time and the percentage of *petite* mutants in liquid culture were significantly affected. The generation of *petite* mutants is usually observed in strains altered in ATP synthase subunits (*48*). The low oligomycin-sensitive ATPase activity of *4*Δ(47–55) mitochondria indicates a strong alteration of the interaction between F_1 and F_o and/or of the oligomycin binding site. On the other hand, shorter deletions did not significantly alter either the generation time or the mitochondrial ATPase activity. Indeed, the ATP synthase activity of the strain *4*Δ(49–55) was identical to that of the wild type with ATP/O ratios of 0.96 and 0.97 for the wild-type and *4*Δ(49–55) mitochondria, respectively.

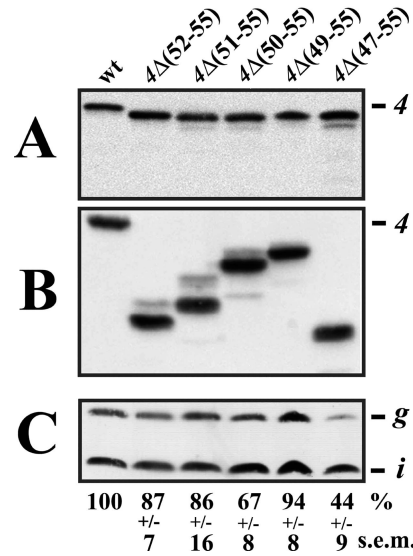

FIGURE 2: Behavior of subunits *4* and mitochondrial content in ATP synthase subunit *g* in mutant mitochondria. Forty micrograms of mitochondrial proteins of PVY162, *4*Δ(52–55), *4*Δ(51–55), *4*Δ(50–55), *4*Δ(49–55), and *4*Δ(47–55) strains were dissociated and submitted to electrophoresis according to Schägger and von Jagow (*42*) (A and C) or Laemmli (*41*) (B). The slab gels were transferred to nitrocellulose, and the blots were incubated with polyclonal antibodies raised against subunits *4* (A and B) and *i* and *g* (C). PVY162 was the control strain. The percentage (%) of remaining subunit *g* was corrected with the respective amounts of subunit *i* in PVY162 and mutant mitochondria. sem: standard error of the mean for four independent experiments.

As a control experiment strain *4*ΔTM1 harboring a subunit *4* devoid of its first 43 amino acid residues displayed a generation time similar to that of the control strain and an oligomycin-sensitive ATPase activity similar to that of the deletion mutants but the *4*Δ(47–55) strain.

Alteration of Subunit 4 and the Presence of the g-Subunit. Two distinct SDS−PAGE systems were used to analyze mutant subunits *4* in Western blot experiments (Figure 2). The five shortened subunits *4* ran faster than the wild-type subunit *4*, to a similar relative molecular mass when using Schägger and von Jagow's electrophoretic system (*42*) (Figure 2A). In Laemmli's SDS gel system (*41*) the relative molecular masses of the mutated subunits *4* were clearly not dependent on the length of the deletion since the subunit *4* harboring the smallest deletion [*4*Δ(52–55)] ran faster than the subunit *4*Δ(49–55) (Figure 2B). Most probably secondary and/or tertiary structures of mutant subunits *4* were still present and not abolished in Laemmli's electrophoretic system, which resulted in an alteration of their migration. This intriguing point has not been further investigated. Since an interaction has been proposed between subunits *4* and *g*, Western blot analyses of solubilized mitochondria were performed to look for the presence of subunit *g* (Figure 2C). Using subunit *i* as reference, we measured a 50% decrease in the amount of subunit *g* in *4*Δ(47–55) mitochondria whereas *4*Δ(49–55) mitochondria did not display such a decrease. We have previously reported that *4*ΔTM1 mitochondria, which harbor a subunit *4* devoid of its first 43 amino acid residues, are nearly fully devoid of subunit *g* (*32*).

CN-PAGE Analyses of ATP Synthase Oligomerization. CN-PAGE was performed to analyze supramolecular species of wild-type and mutant ATP synthases (Figure 3). Oligo-

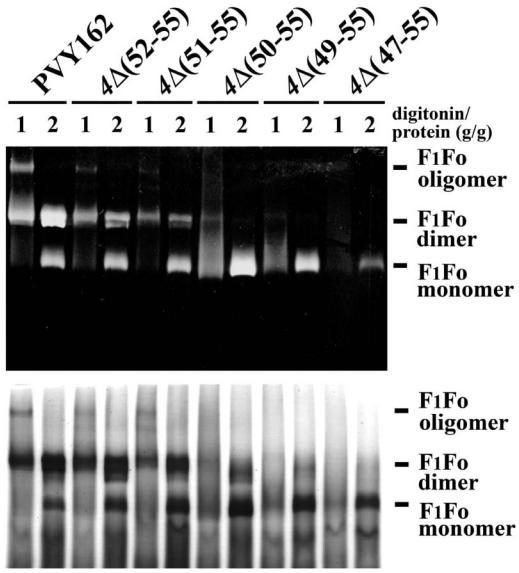

FIGURE 3: Destabilization of the oligomeric forms of the ATP synthase by alteration of subunit *4* loop 47–55 located in the intermembrane space. Mitochondria (0.5 mg of protein) from the indicated strains were incubated with 50 μL of a digitonin solution at the indicated digitonin to protein ratios. After centrifugation, aliquots of the each supernatant containing 150 μg of proteins were loaded onto a 3–13% polyacrylamide slab gel. After CN-PAGE analysis, the bands were revealed by ATPase activity assay (top panel) and Coomassie Blue staining (lower panel). PVY162 was the control strain.

meric and dimeric species of ATP synthase were observed upon solubilization of yeast mitochondria with digitonin at a detergent/protein ratio of 1 (g/g). When the ratio was increased to 2 (g/g), the enzyme was dimeric and monomeric. When analyzing ATP synthases altered in the subunit *4* intermembrane space loop, the larger the deletion was, the less oligomeric and dimeric forms were observed in the native gel (Figure 3). As estimated by the CN-PAGE, the ATPase activity associated to intact ATP synthase was reduced for the *4*Δ(47–55) mitochondria. Such a decrease was not found in the standard activity test (Table 1). This discrepancy is interpreted by the different assay conditions (in gel activity over hours after digitonin solubilization or activity measurement over minutes in the presence of Triton X-100) and the presence of altered F_1F_o-ATP synthase in *4*Δ(47–55) mitochondria.

In CN-PAGE experiments, using detergent/protein ratios of 2 (g/g), ATP synthase extracted from *4*Δ(50–55), *4*Δ(49–55), and *4*Δ(47–55) mitochondria ran as exclusively as monomers. This phenotype has been observed in the mutated yeast strains Δ*g*, Δ*e*, and *4*ΔTM1 and strains altered in the GxxxG dimerization motifs of *e*- and *g*-subunits (*11, 32, 49–51*). In these mutant cells subunit *g* is recurrently absent of mitochondria. We focused on the deletion *4*Δ(49–55) because it did not perturb the amount of subunit *g* whereas the mutated ATP synthase was no more dimeric in native gel experiments. Arnold et al. (*11*) have shown that subunits *e*, *g*, and *k* were specifically associated with the dimeric forms of the F_oF_1-ATP synthase. To examine the behavior of these subunits in the absence of ATP synthase dimerization, CN-PAGE followed by SDS−PAGE analyses were carried out on wild-type and *4*Δ(49–55) mitochondrial digitonin extracts (Figure 4). The blots were probed with antibodies raised against subunits *i*, *g*, *e*, and *k*. We confirmed that subunits *e*, *g*, and *k* were absent from the monomeric form of the wild-type ATP synthase (Figure 4A,C) and showed that these subunits were associated with the monomeric form of the mutant enzyme in digitonin extracts (Figure 4B,D). A similar experiment with a BN-PAGE as the first dimension showed a partial dissociation of subunits *g* and *e* from the monomeric mutant ATP synthase, running in the front of the native gel (not shown). This observation reminds the destabilizing effect of the Coomassie Brilliant Blue G250 on oligomeric ATP synthases (*12*). We conclude that mutating the loop of subunit *4* promotes a lack of dimerization of the ATP synthase that is not linked to the absence of subunit *g*, nor to the release of subunits *e*, *g*, or *k* from the complex after solubilization by the detergent.

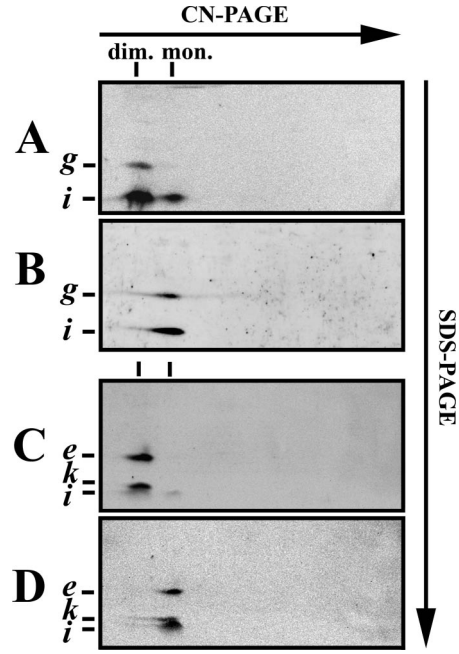

FIGURE 4: Subunits *g*, *e*, and *k* remain associated to the monomeric form of the ATP synthase in the *4*Δ(49–55) mutant. Mitochondria (0.5 mg of protein) from wild type (A and C) or the *4*Δ(49–55) mutant (B and D) were incubated with 50 μL of a digitonin solution at the detergent to protein ratio of 2 g/g. After centrifugation, aliquots of the supernatant containing 150 μg of proteins were analyzed by CN-PAGE. A lane was cut, incubated with SDS, submitted to an SDS−PAGE, and analyzed by Western blot. Polyclonal antibodies against subunits *i* and *g* were used to probe the blots (A and B). In a second step, the blots were stripped and probed again with antibodies against subunits *i*, *e*, and *k* (C and D).

Cysteines 4N25C, gC75, 6C23, and eC28 as Targets of Disulfide Bridge Formation. In a previous work we have shown the proximity of subunits *4* and *g* since, after insertion of a unique cysteine in subunit *4*, it was possible to perform a cross-link between the unique cysteine residue of subunit *g* (C75) and either *4*K7C or *4*K14C by using *N*,*N*′-(1,2-phenylene)dimaleimide (*32*). We show here that such a heterodimerization also occurred by oxidation between *4*N25C and *g*C75, thus confirming the proximity between the two subunits. We took advantage of this result to determine the neighboring of mutant subunits *4* (Figure 5). Mitochondria (top panel) and Triton X-100 mitochondrial extracts (lower panel) of strains bearing a cysteine residue in position 25 of subunit *4* and deleted or not in the loop 47–55 were submitted to oxidation and analyzed by Western blot. The *4* + *g* heterodimerization was clearly dramatically

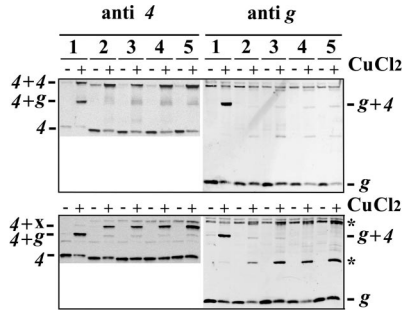

FIGURE 5: Loss of heterodimerization between subunits *4* and *g* upon deletion in loop 47–55 of subunit *4*. Mitochondria (top panel) and mitochondrial Triton X-100 extracts (lower panel) of *4*N25C, *4*Δ(52–55)-N25C, *4*Δ(51–55)-N25C, *4*Δ(50–55)-N25C, and *4*Δ(49–55)-N25C strains (lanes 1, 2, 3, 4, and 5, respectively) were incubated or not with 1 mM $CuCl_2$ at 4 °C for 30 min. The reaction was stopped by addition of 5 mM EDTA and 5 mM NEM. Samples (40 μg of protein) were dissociated with SDS, separated in SDS−PAGE according to Schägger and von Jagow (*42*), and analyzed by Western blot. The blots were incubated with polyclonal antibodies raised against either subunit *4* or subunit *g*. *, nonidentified cross-linked products.

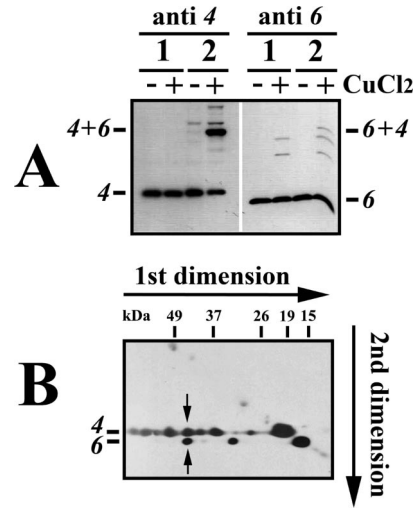

FIGURE 6: Involvement of *4*N25C and *6*C23 in a cross-link between subunits *4* and *6*. Mitochondrial Triton X-100 extracts of *4*Δ(49–55) (lanes 1) and *4*Δ(49–55)-N25C (lanes 2) strains were incubated or not with 1 mM $CuCl_2$ as in Figure 5. Samples were separated in SDS−PAGE according to Schägger and von Jagow (*42*) and analyzed by Western blot with antibodies raised against either subunit *4* or subunit *6* (A). A lane of the SDS slab gel corresponding to the same experiment with Δ(49–55)-N25C mitochondria after $CuCl_2$ oxidation was cut (first dimension), incubated with β-mercaptoethanol, and submitted to a second dimension. The slab gel was transferred to nitrocellulose, and the blot was incubated simultaneously with antibodies raised against subunit *4* and against subunit *6* (B). The arrows indicate the positions of subunits *4* and *6*.

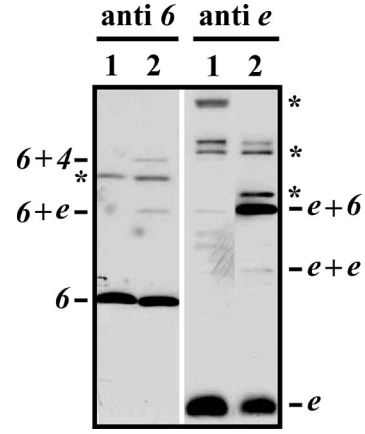

FIGURE 7: Appearance of an *e* + *6* heterodimer upon deletion in loop 47–55 of subunit *4*. Mitochondrial Triton X-100 extracts of *4*N25C (lanes 1) and Δ(49–55)-N25C (lanes 2) strains were incubated or not with 1 mM $CuCl_2$, and the Western blot experiment was done as in Figure 5, with antibodies raised against either subunit *6* (left panel) or subunit *e* (right panel). *, nonidentified cross-linked products.

decreased in mutant mitochondria, hence indicating an altered face-to-face pairing between *g*C75 and *4*N25C when the intermembrane space loop of subunit *4* is altered. Additional cross-links were observed. Among them, the oxidation-dependent dimerization of subunit *4* in mitochondrial membranes has been already depicted (*24*). More surprising was the presence of a cross-linked product (*4* + X) in Triton X-100 mitochondrial extracts of all mutant strains. This adduct was identified by two means as a *4* + *6* heterodimer. First, the antibody raised against subunit *6* recognized a cross-linked product that was strictly dependent on the cysteine residue introduced in position 25 of subunit *4* (Figure 6A). Second, the same experiment was repeated, and the gel slice was incubated with β-mercaptoethanol to cleave the disulfide bond generated by oxidation. The proteins were separated in a second dimension and analyzed by Western blot, with anti-*4* and anti-*6* antibodies (Figure 6B). The experiment showed that spots corresponding to subunits *4* and *6* migrated from the same initial spot in the first dimension, thus confirming the existence of a *4* + *6* cross-link. In oxidized *4*Δ(49–55)-N25C Triton X-100 extracts, besides this *6* + *4* heterodimer, another cross-link product involving subunit *6* was also revealed by anti-*e* antibody (Figure 7). This *e* + *6* heterodimer involves the unique cysteine residue of subunit 6 (*6*C23) and the unique residue of subunit *e* (*e*C28), both located on the outer side of the inner mitochondrial membrane. It indicates that the two cysteine residues are closer in the *4*Δ(49–55) Triton X-100 extract than in the wild type. Altogether, these data show that deleting loop 47–55 modified the neighborhood of residues *4*N25C, *g*C75, *6*C23, and *e*C28 (at least in the detergent extract).

Mitochondrial Morphology. The involvement of ATP synthase oligomerization in the mitochondrial morphology has been largely documented (*19, 24, 31, 32, 50–52*). Using transmission electron microscopy, mitochondria of wild-type cells appear mainly as ovoid objects of 400–600 nm in diameter. Mitochondria in *4*Δ(52–55) (Figure 8A) and in *4*Δ(51–55) strains (not shown) are identical to those of wild-type cells. In these organelles, cristae are mainly found in the vicinity of the peripheral inner mitochondrial membrane and are heavily packed with a narrow intermembrane space (Figure 8A). Transmission electron microscopy experiments conducted on *4*Δ(47–55) cells revealed a majority of mitochondria with "onion-like" structure (Figure 8D). Occurrence of these structures may be correlated with the 50% decrease in the amount of subunit *g* in *4*Δ(47–55) mitochondria (Figure 2C), as previously reported (*31*). The *4*Δ(49–55) and *4*Δ(50–55) mutants were less affected but displayed long inner membrane structures traversing elongated organelles. In addition, the cristae were frequently pinched (arrows in Figure 8B,C), and the intermembrane space appeared larger than that of wild-type cristae.

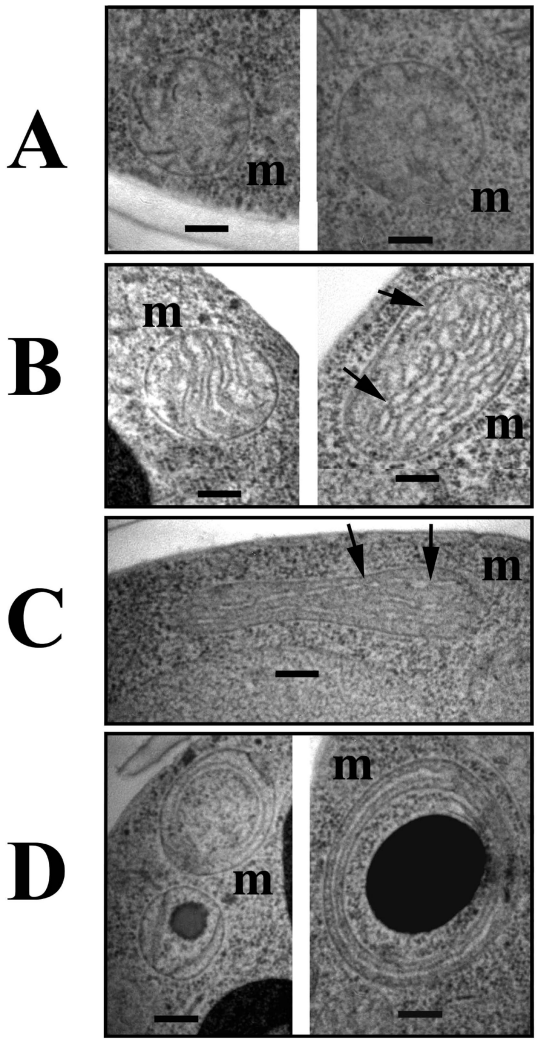

FIGURE 8: Transmission electron microscopy of yeast mutant cells: *4*Δ(52–55) (A), *4*Δ(50–55) (B), *4*Δ(49–55) (C), and *4*Δ(47–55) (D). The bars indicate 200 nm. m = mitochondria. The black arrows indicate spots where membranes of cristae are joined.

DISCUSSION

A recurrent point emerging from published data is that the presence of both subunits *e* and *g* in mitochondria is required to maintain the association of ATP synthases in detergent extracts and is necessary for the maintenance of the mitochondrial morphology (*11, 24–26, 31*). Subunit *e* is indispensable for the correct assembly of subunit *g* in mitochondria, and the rate of subunit *g* degradation is increased in mutants lacking the coiled-coil domains of subunit *e* (*52*). Similarly, in the strain *4*ΔTM1 where the whole N-terminal domain of subunit *4* (containing TM1) is deleted, subunit *g* is nearly absent of mitochondria (*32*). On the other hand, in Δ*g* and *4*ΔTM1 strains, subunit *e* is present in normal amount (*32, 53*). These subunits seem to interact with one another at the dimerization interface level of ATP synthases since heterodimers *e* + *g* or *g* + *4* have been obtained after cross-linking experiments (*32, 49, 50*). While apparently present at the dimerization interface, subunit *k* is not indispensable for dimer stability (*11*). How these subunits are arranged and participate in the dimerization interface is a key issue for understanding the oligomerization phenomenon. Whereas previous studies reported an instability of yeast ATP synthase oligomers associated with the loss of subunit *g* in mitochondria, here we show a full loss of supramolecular structures of the ATP synthase occurring while subunit *g* content in mitochondria is unaffected. While the deletion through amino acid residues 49 and 55 has little effect on ATP synthase function, the association between monomers is dramatically altered at least in detergent extracts, as shown by native gel electrophoresis. The instability observed in detergent extract is not due to the release of subunits *g*, *e*, or *k* from the F_oF_1-ATP synthase, as shown by their association with monomeric ATP synthase in two-dimensionnal CN/SDS−PAGE experiments. However, BN-PAGE experiments show partial dissociation of subunits *g*, *e*, or *k* when the *4*-subunit loop is deleted (not shown). The same behavior has been observed for subunit *e* when mutated in its GxxxG motif (*51*).

To get further molecular details at the dimerization interface, cross-linking experiments were conducted using endogenous and/or inserted unique cysteine residues in subunits *4*, *g*, *e*, and *6*. All of these components are transmembranous proteins, located in the F_o domain of ATP synthase. In the wild-type enzyme, the concerned cysteine residues are located close to or at the water−membrane interface, in the mitochondrial matrix (residues *4*N25C and *g*C75) or in the intermembrane space (residues *e*C28 and *6*C23) (*22, 47, 50*). We focused on the *4*Δ(49–55) strain, for which dimerization of ATP synthase is dramatically altered while subunit *g* content in mitochondria is normal. In this strain, modifications of the cross-linking profile were observed: lack of cross-linking between positions *4*N25C and *g*C75, appearance of a cross-linking product between *4*N25C and *6*C23, and another one involving *6*C23 and *e*C28. The *4* + *6* heterodimer was only observed in detergent extracts of mutant ATP synthases. This was striking because such an adduct must involve one cysteine residue located in the matrix space (*4*N25C) and the other one in the intermembrane space (*6*C23). The shortening of loop 47–55 presumably leads to a knocking over of the subunit *4* N-terminal domain (including the first membrane-spanning segment) on the opposite side of the F_1 domain, but only in the digitonin extract. This should explain the loss of supramolecular species of the ATP synthase in native PAGE experiments. Altogether, these results illustrate the importance of hydrophilic loop 47–55 of subunit *4* for positioning its own flanking TM domains (i.e., domains *4*TM1 and/or *4*TM2) and/or other polypeptidic chains belonging to the F_o domain. The major contact site between two monomers in dimeric ATP synthases from different species has been recurrently identified as the F_o part of the complex (*14–16*). Furthermore, the contribution of subunits *e* and *g* to the dimeric interface relies on the conserved GxxxG motif found inside their TM domain (*49–51*). We propose that the hydrophilic intermembrane space loop of subunit *4* is an indispensable motif for the formation of a strong dimerization interface in the hydrophobic core of the ATP synthase. In a previous paper we have hypothesized that the first transmembrane segment of subunit *4*, TM1, could hold the interaction with subunit *g* (*32*). In fact, large deletions inside TM1 [*4*Δ(25–30), *4*Δ(31–36), and *4*Δ(38–44)] did not fully destabilize the supramolecular structures of the ATP synthase (unpublished data). Compared with the full loss of dimeric ATP synthase when deletions are introduced in the more hydrophilic loop, this result indicates that TM1 is less important for the dimeric

interface than the adjacent loop. This conclusion correlates with the fact that the most conserved residues among the *b*-subunits from different species are located in the hydrophilic loop at positions 47, 51, and 55 [numbering of yeast subunit *4* (Figure 1)] but not in the hydrophobic TM1.

Deletions in the intermembrane space loop of subunit *4* alters the mitochondrial morphology despite the presence of subunits *g* and *e*. Interestingly, mitochondria of *4*Δ(50–55) and *4*Δ(49–55) mutant strains display cristae morphologies resembling those observed when subunits *e* or *g* are partially depleted from mitochondria (*31*). They correspond to an intermediary step between "normal" and onion-like mitochondria. As revealed by electron tomography, normal yeast cristae consist of a rather curved membrane (*54*). The reorganized cristae in onion-like structures appear as long flat pairs of two membranes separated by a constant distance (*24*). The transition from normal to onion-like topology is interpreted as a lamellarization of the inner membrane. Furthermore, the intracristal space width is apparently increased concomitant with such a deformation. This phenotype results either from the loss of supramolecular forms of the ATP synthase (*24*) or from cross-links between adjacent ATP synthases (*19*), pointing out that a correct arrangement and/or the dynamics of oligomeric ATP synthase seem to be important for cristae morphology. The yeast mutants described here show an inverse correlation between the decreasing stability of supramolecular forms of the ATP synthase in native PAGE (Figure 3) and the lamellarization of the inner membrane (Figure 8). Our data favor the idea that the strength of cohesion of oligomeric ATP synthases could drive the bending of the membrane. Loop 47–55 of subunit *4* is actively involved in such a process.

ACKNOWLEDGMENT

The authors are grateful to Dr. Christine Schwimmer for reading the English version of the manuscript and Dr. Rosemary Stuart for the gift of anti-*k*-subunit antibody.

REFERENCES

1. Fillingame, R. H. (1999) Molecular rotary motors. *Science 286*, 1687–1688.
2. Pedersen, P. L., Ko, Y. H., and Hong, S. (2000) ATP synthases in the year 2000: evolving views about the structures of these remarkable enzyme complexes. *J. Bioenerg. Biomembr. 32*, 325–332.
3. Stock, D., Gibbons, C., Arechaga, I., Leslie, A. G. W., and Walker, J. E. (2000) The rotary mechanism of ATP synthase. *Curr. Opin. Struct. Biol. 10*, 672–679.
4. Senior, A. E., Nadanaciva, S., and Weber, J. (2002) The molecular mechanism of ATP synthesis by F1F0-ATP synthase. *Biochim. Biophys. Acta 1553*, 188–211.
5. Dickson, V. K., Silvester, J. A., Fearnley, I. M., Leslie, A. G., and Walker, J. E. (2006) On the structure of the stator of the mitochondrial ATP synthase. *EMBO J. 25*, 2911–2918.
6. Abrahams, J. P., Leslie, A. G. W., Lutter, R., and Walker, J. E. (1994) Structure at 2.8 Å resolution of F1-ATPase from bovine heart mitochondria. *Nature 370*, 621–628.
7. Bianchet, M. A., Hullihen, J., Pedersen, P. L., and Amzel, L. M. (1998) The 2.8-Å structure of rat liver F1-ATPase: configuration of a critical intermediate in ATP synthesis/hydrolysis. *Proc. Natl. Acad. Sci. U.S.A. 95*, 11065–11070.
8. Hausrath, A. C., Grüber, G., Matthews, B. W., and Capaldi, R. A. (1999) Structural features of the gamma subunit of the *Escherichia coli* F(1) ATPase revealed by a 4.4-Å resolution map obtained by x-ray crystallography. *Proc. Natl. Acad. Sci. U.S.A. 96*, 13697–13702.
9. Gibbons, C., Montgomery, M. G., Leslie, A. G. W., and Walker, J. E. (2000) The structure of the central stalk in bovine F(1)-ATPase at 2.4 Å resolution. *Nat. Struct. Biol. 7*, 1055–1061.
10. Stock, D., Leslie, A. G. W., and Walker, J. E. (1999) Molecular architecture of the rotary motor in ATP synthase. *Science 286*, 1700–1705.
11. Arnold, I., Pfieffer, K., Neupert, W., Stuart, R. A., and Schägger, H. (1998) Yeast mitochondrial F1F0-ATP synthase exists as a dimer: identification of three dimer-specific subunits. *EMBO J. 17*, 7170–7178.
12. Krause, F., Reifschneider, N. H., Goto, S., and Dencher, N. A. (2005) Active oligomeric ATP synthases in mammalian mitochondria. *Biochem. Biophys. Res. Commun. 329*, 583–590.
13. Eubel, H., Jansch, L., and Braun, H. P. (2003) New insights into the respiratory chain of plant mitochondria. Supercomplexes and a unique composition of complex II. *Plant Physiol. 133*, 274–286.
14. Minauro-Sanmiguel, F., Wilkens, S., and Garcia, J. J. (2005) Structure of dimeric mitochondrial ATP synthase: Novel F0 bridging features and the structural basis of mitochondrial cristae biogenesis. *Proc. Natl. Acad. Sci. U.S.A. 102*, 12356–12358.
15. Dudkina, N. V., Heinemeyer, J., Keegstra, W., Boekema, E. J., and Braun, H. P. (2005) Structure of dimeric ATP synthase from mitochondria: an angular association of monomers induces the strong curvature of the inner membrane. *FEBS Lett. 579*, 5769–5772.
16. Dudkina, N. V., Sunderhaus, S., Braun, H. P., and Boekema, E. J. (2006) Characterization of dimeric ATP synthase and cristae membrane ultrastructure from *Saccharomyces* and *Polytomella* mitochondria. *FEBS Lett. 580*, 3427–3432.
17. Spannagel, C., Vaillier, J., Arselin, G., Graves, P. V., Grandier-Vazeille, X., and Velours, J. (1998) Evidence of a subunit 4 (subunit b) dimer in favor of the proximity of ATP synthase complexes in yeast mitochondrial membrane. *Biochim. Biophys. Acta 1414*, 260–264.
18. Paumard, P., Arselin, G., Vaillier, J., Chaignepain, S., Bathany, K., Schmitter, J. M., Brèthes, D., and Velours, J. (2002) Two ATP synthases can be linked through subunits i in the inner mitochondrial membrane of *Saccharomyces cerevisiae*. *Biochemistry 41*, 10390–10396.
19. Gavin, P. D., Prescott, M., Luff, S. E., and Devenish, R. J. (2004) Cross-linking ATP synthase complexes in vivo eliminates mitochondrial cristae. *J. Cell. Sci. 117*, 2333–2343.
20. Buzhynskyy, N., Sens, P., Prima, V., Sturgis, J. N., and Scheuring, S. (2007) Rows of ATP synthase dimers in native mitochondrial inner membranes. *Biophys. J. 93*, 2870–2876.
21. Collinson, I. R., Runswick, M. J., Buchanan, S. K., Fearnley, I. M., Skehel, J. M., van Raai, M. J., Griffiths, D. E., and Walker, J. E. (1994) Fo membrane domain of ATP synthase from bovine heart mitochondria: purification, subunit composition, and reconstitution with F1-ATPase. *Biochemistry 33*, 7971–7978.
22. Arnold, I., Bauer, M. F., Brunner, M., Neupert, W., and Stuart, R. A. (1997) Yeast mitochondrial F1F0-ATPase: the novel subunit e is identical to Tim11. *FEBS Lett. 411*, 195–200.
23. Velours, J., and Arselin, G. (2000) The *Saccharomyces cerevisiae* ATP synthase. *J. Bioenerg. Biomembr. 32*, 383–390.
24. Paumard, P., Vaillier, J., Coulary, B., Schaeffer, J., Soubannier, V., Mueller, D. M., Brèthes, D., di Rago, J. P., and Velours, J. (2002) The ATP synthase is involved in generating mitochondrial cristae morphology. *EMBO J. 21*, 221–230.
25. Gavin, P. D., Prescott, M., and Devenish, R. J. (2005) F1F0-ATP synthase complex interactions in vivo can occur in the absence of the dimer specific subunit e. *J. Bioenerg. Biomembr. 37*, 55–66.
26. Fronzes, R., Weimann, T., Vaillier, J., Velours, J., and Brèthes, D. (2006) The peripheral stalk participates in the yeast ATP synthase dimerization independently of e and g subunits. *Biochemistry 45*, 6715–6723.
27. García, J. J., Morales-Ríos, E., Cortés-Hernandez, P., and Rodríguez-Zavala, J. S. (2006) The inhibitor protein (IF1) promotes dimerization of the mitochondrial F1F0-ATP synthase. *Biochemistry 45*, 12695–12703.
28. Dienhart, M., Pfeiffer, K., Schagger, H., and Stuart, R. A. (2002) Formation of the yeast f1f0-ATP synthase dimeric complex does not require the ATPase inhibitor protein, inh1. *J. Biol. Chem. 277*, 39289–39295.
29. Allen, R. D., Schroeder, C. C., and Fok, A. K. (1989) An investigation of mitochondrial inner membranes by rapid-freeze deep-etch techniques. *J. Cell Biol. 108*, 2233–2240.
30. Allen, R. D. (1995) Membrane tubulation and proton pumps. *Protoplasma 189*, 1–8.

31. Arselin, G., Vaillier, J., Salin, B., Schaeffer, J., Giraud, M. F., Brèthes, D., and Velours, J. (2004) The modulation in subunits e and g amounts of yeast ATP synthase modifies mitochondrial cristae morphology. *J. Biol. Chem. 279*, 40392–40399.
32. Soubannier, V., Vaillier, J., Paumard, P., Coulary, B., Schaffer, J., and Velours, J. (2002) In the absence of the first membrane-spanning segment of subunit 4. (b), the yeast ATP synthase is functional but does not dimerize or oligomerize. *J. Biol. Chem. 277*, 10739–10745.
33. Kun, E., Kirsten, E., and Piper, W. N. (1979) Stabilization of mitochondrial functions with digitonin. *Methods Enzymol. 55*, 115–118.
34. Güldener, U., Heck, S., Fielder, T., Beinhauer, J., and Hegemann, J. H. (1996) A new efficient gene disruption cassette for repeated use in budding yeast. *Nucleic Acids Res. 24*, 2519–2524.
35. Paul, M. F., Guérin, B., and Velours, J. (1992) The C-terminal region of subunit 4 (subunit b) is essential for assembly of the F0 portion of yeast mitochondrial ATP synthase. *Eur. J. Biochem. 205*, 163–172.
36. Arselin de Chateaubodeau, G., Guérin, M., and Guérin, B. (1976) Permeability of yeast mitochondrial internal membrane: structure-activity relationship. *Biochimie (Paris) 58*, 601–610.
37. Guérin, B., Labbe, P., and Somlo, M. (1979) Preparation of yeast mitochondria (*Saccharomyces cerevisiae*) with good P/O and respiratory control ratios. *Methods Enzymol. 55*, 149–159.
38. Lowry, O. H., Rosebrough, N. J., Farr, A. L., and Randall, R. J. (1951) Protein measurement with the Folin phenol reagent. *J. Biol. Chem. 193*, 265–275.
39. Rigoulet, M., and Guérin, B. (1979) Phosphate transport and ATP synthesis in yeast mitochondria: effect of a new inhibitor: the tribenzylphosphate. *FEBS Lett. 102*, 18–22.
40. Velours, J., Vaillier, J., Paumard, P., Soubannier, V., Lai-Zhang, J., and Mueller, D. M. (2001) Bovine coupling factor 6, with just 14.5% shared identity, replaces subunit h in the yeast ATP synthase. *J. Biol. Chem. 276*, 8602–8607.
41. Laemmli, U. K. (1970) Cleavage of structural proteins during the assembly of the head of bacteriophage T4. *Nature 227*, 680–685.
42. Schägger, H., and von Jagow, G. (1987) Tricine-sodium dodecyl sulfate-polyacrylamide gel electrophoresis for the separation of proteins in the range from 1 to 100 kDa. *Anal. Biochem. 166*, 368–379.
43. Arselin, G., Vaillier, J., Graves, P. V., and Velours, J. (1996) ATP synthase of yeast mitochondria. Isolation of the subunit h and disruption of the ATP14 gene. *J. Biol. Chem. 271*, 20284–20290.
44. Schägger, H., Cramer, W. A., and von Jagow, G. (1994) Analysis of molecular masses and oligomeric states of protein complexes by blue native electrophoresis and isolation of membrane protein complexes by two-dimensional native electrophoresis. *Anal. Biochem. 217*, 220–230.
45. Yoshida, M., Sone, N., Hirata, H., and Kagawa, Y. (1975) A highly stable adenosine triphosphatase from a thermophillie bacterium. Purification, properties, and reconstitution. *J. Biol. Chem. 250*, 7910–7916.
46. Grandier-Vazeille, X., and Guérin, M. (1996) Separation by blue native and colorless native polyacrylamide gel electrophoresis of the oxidative phosphorylation complexes of yeast mitochondria solubilized by different detergents: specific staining of the different complexes. *Anal. Biochem. 242*, 248–254.
47. Spannagel, C., Vaillier, J., Chaignepain, S., and Velours, J. (1998) Topography of the yeast ATP synthase F0 sector by using cysteine substitution mutants. Cross-linkings between subunits 4, 6, and f. *Biochemistry 37*, 615–621.
48. Contamine, V., and Picard, M. (2000) Maintenance and integrity of the mitochondrial genome: a plethora of nuclear genes in the budding yeast. *Microbiol. Mol. Biol. Rev. 64*, 281–315.
49. Saddar, S., and Stuart, R. A. (2005) The yeast F(1)F(0)-ATP synthase: analysis of the molecular organization of subunit g and the importance of a conserved GXXXG motif. *J. Biol. Chem. 280*, 24435–24442.
50. Bustos, D. M., and Velours, J. (2005) The modification of the conserved GXXXG motif of the membrane-spanning segment of subunit g destabilizes the supramolecular species of yeast ATP synthase. *J. Biol. Chem. 280*, 29004–29010.
51. Arselin, G., Giraud, M. F., Dautant, A., Vaillier, J., Brèthes, D., Coulary-Salin, B., Schaeffer, J., and Velours, J. (2003) The GxxxG motif of the transmembrane domain of subunit *e* is involved in the dimerisation/oligomerization of the yeast ATP synthase complex in the mitochondrial membrane. *Eur. J. Biochem. 270*, 1875–1884.
52. Bornhövd, C., Vogel, F., Neupert, W., and Reichert, A. S. (2006) Mitochondrial membrane potential is dependent on the oligomeric state of F1F0-ATP synthase supracomplexes. *J. Biol. Chem. 281*, 13990–13998.
53. Everard-Gigot, V., Dunn, C. D., Dolan, B. M., Brunner, S., Jensen, R. E., and Stuart, R. A. (2005) Functional analysis of subunit e of the F1Fo-ATP synthase of the yeast *Saccharomyces cerevisiae*: importance of the N-terminal membrane anchor region. *Eukaryotic Cell 4*, 346–355.
54. Mannella, C. A., Pfeiffer, D. R., Bradshaw, P. C., Moraru, I. I., Slepchenko, B., Loew, L. M., Hsieh, C. E., Buttle, K., and Marko, M. (2001) Topology of the mitochondrial inner membrane: dynamics and bioenergetic implications. *IUBMB Life 52*, 93–100.

BI702000G